University of Massachusetts Medical School
eScholarship@UMMS

GSBS Dissertations and Theses | Graduate School of Biomedical Sciences

10-2010

Generating Nucleosomal Asymmetry in Saccharomyces cerevisiae: A Masters Thesis

Yuanyuan Chen
University of Massachusetts Medical School, Yuanyuan.Chen@umassmed.edu

Follow this and additional works at: http://escholarship.umassmed.edu/gsbs_diss

 Part of the Genetics and Genomics Commons, and the Medicine and Health Sciences Commons

Recommended Citation
Chen, Yuanyuan, "Generating Nucleosomal Asymmetry in Saccharomyces cerevisiae: A Masters Thesis" (2010). University of Massachusetts Medical School. *GSBS Dissertations and Theses.* Paper 500.
http://escholarship.umassmed.edu/gsbs_diss/500

This material is brought to you by eScholarship@UMMS. It has been accepted for inclusion in GSBS Dissertations and Theses by an authorized administrator of eScholarship@UMMS. For more information, please contact Lisa.Palmer@umassmed.edu.

GENERATING NUCLEOSOMAL ASYMMETRY IN *SACCHAROMYCES CEREVISIAE*

A Masters Thesis Presented

by

YUANYUAN CHEN

Submitted to the Faculty of the University of Massachusetts Graduate School
of Biomedical Sciences, Worcester
in partial fulfillment of the requirements for the degree of

MASTER OF SCIENCE

October, 2010

GENE FUNCTION AND EXPRESSION

GENERATING NUCLEOSOMAL ASYMMETRY

IN *SACCHAROMYCES CEREVISIAE*

A Masters Thesis Presented

By

YUANYUAN CHEN

The signatures of the Master's Thesis Committee signifies completion and approval as to style and content of the Thesis

Craig L. Peterson, Chair of Committee

Rando Oliver, Member of Committee

Dan Bolon, Member of Committee

Job Dekker, Member of Committee

The signature of the Dean of the Graduate School of Biomedical Sciences signifies that the student has met all master's degree graduation requirements of the school.

Anthony Carruthers, Ph.D.,
Dean of the Graduate School of Biomedical Sciences

Interdisciplinary Graduate Program

October, 2010

Acknowledgements

I wish to express my sincere thanks to all the people who have helped me during my three years at University of Massachusetts Graduate School of Biomedical Sciences. Thank Paul, for his continuous guidance, patience, encouragement, support and understanding. He is a great mentor full of enthusiasm for research. Thank all lab members, Eric, Jessica, Corey, Amie, Toshi and Judy, for their kindness, help and friendship. Thank all my committee members, Craig, Dan, Ollie and Job, for their time and energy paid for directing my qualifying exam and research.

For the studies carried in this thesis, special thanks to Dan, for his protein design and random mutagenesis protocol; thank Jeremy from Rando lab, for construction of some plasmids and microarray experiment; and thank Paul, for sequencing of the isolates from genetic screening and mutagenesis of the *Rtt109* alleles. Without these help the projects wouldn't have gone so far.

Table of Contents

Abstract

There are two copies of each core histone in a nucleosome, however, it is unclear whether post-translational modifications on each molecule function redundantly or if symmetrical modifications are required to properly regulate gene expression. We tried to address this question by breaking nucleosomal symmetry and measuring its impact on gene expression. Our strategy includes re-engineering specific residues at the H3-H3 interface, generating pairs of mutant proteins, which were predicted by computational methods to form obligate heterodimers. Using *S. cerevisiae* as a model system, we tested the viability of strains with mutant histones, and analyzed the interaction between by co-immunoprecipitation from mononucleosome preparations. We also measured the changes of gene expression in the strains bearing single-tailed or tailless H3 heterodimers. The data suggested that the best computationally-derived H3 pair was *frequently*, but not exclusively heterodimeric *in vivo*. In order to obtain a more stringent H3 heterodimer, random mutagenesis was performed on four codons in the original computational design, and then genetic screening of the mutant libraries was performed.

List of Tables and Figures

List of Third Party Copyrighted Material

Figure Number	Publisher / Author
Figure 1.1	Garland Science Publishing
Figure 3.1	Dan Bolon
Figure 3.7	Oliver Rando

CHAPTER I Introduction

The basic building block of eukaryotic chromatin is the nucleosome, which consists of 147 bp of DNA wrapped around an octamer of core histones -- a $(H3/H4)_2$ tetramer flanked by two H2A/H2B dimers (Luger et al., 1997). H3/H4 form a dimer through a “handshake” interaction as well as H2A/H2B, and then two H3/H4 pairs interact via a H3-H3 four-helix bundle to form a H3/H4 tetramer (Figure 1.1). Each of the two H2A-H2B dimers is added onto the H3/H4 tetramer through the interaction between the histone folds of H2B and H4 to form an intact histone octamer. In addition to its histone fold, each of the core histones has a long N-terminal amino acid ‘tail’, which extends out from the DNA-histone core (Figure 1.1). The H3-H3 four-helix bundle contains hydrogen bonds of buried charged groups and several hydrophobic bonds forming intermolecular interaction. The overall conformation of H2B-H4 interface is closely related to that of H3-H3, except with increased hydrophobic contribution (Luger et al., 1997).

Each of the histone proteins can be post-translationally modified, particularly in the N-terminal tail domains. At least eight distinct types of modifications have been found on histones, including the well-known small covalent modifications, such as acetylation, methylation and phosphorylation. These histone modifications regulate diverse processes involving chromatin dynamics, such as gene activity, replication, DNA repair, gene silencing, genomic stability and apoptosis (Millar and Grunstein, 2006).

“Crosstalk” among histone modifications occurs at several aspects (Suganuma and Workman, 2008). One aspect is that the first modification can promote the generation of another within the same or between different histones. For example, in *Saccharomyces cerevisiae*, H3K36 methylation by the Pol II-associated Set2 targets H3/H4 deacetylation by the Rpd3S after the passage of RNA polymerase, to suppress intragenic transcription initiation (Carrozza et al., 2005); H2B mono-ubiquitination by Rad6 is required for H3K4 methylation by Set1 and H3K79 methylation by Dot1 (Lee et al., 2007). The second aspect is that many histone modifying complexes contain more than one enzymes, which need to work together to coordinate histone modification. The third aspect involves connecting histone modifications to H3 tail clipping. In *S. cerevisiae*, a H3 endopeptidase tail-clipping activity (N terminal cleavage after Ala21) was identified, which has a preference for tails carrying repressive modifications associated with promoters (Santos-Rosa et al., 2009). It follows transcription induction and precedes nucleosome eviction, and uncleavable H3 mutant impaired gene expression. All these examples of crosstalk indicate that histone modifications are not independent or simply additive, but inter-linked and cooperative.

Most of previous studies (*in vivo*) on histone modifications ignored the presence of two copies of each core histone in the nucleosome. They either were unable to distinguish if one or both copies of histones were modified, or only focused on nucleosomes with both copies of histone containing the same

mutations. Hence it is an interesting question to ask whether histone modifications on the two copies function redundantly or both (symmetric modifications) are required for regulating any gene expression during the whole cell cycle. Our strategy to address this question is to generate an obligate H3 heterodimer, so that different mutations could be made on the two H3 tails asymmetrically within each nucleosome. By measuring its impact on gene expression, we could tell whether a single copy of histone modifications is sufficient for proper regulation or not.

Figure 1.1 The assembly of a histone octamer. The histone H3/H4 dimer and the H2A/H2B dimer are formed from the handshake interaction. An H3/H4 tetramer forms the scaffold of the octamer onto which two H2A-H2B dimers are added, to complete the assembly. The histones are colored as shown. All eight N-terminal tails of the histones protrude from the disc-shaped core structure. The H3-H3 interface consists of a bundle of four alpha helices, circled in red. This holds together the two halves of the histone tetramer.

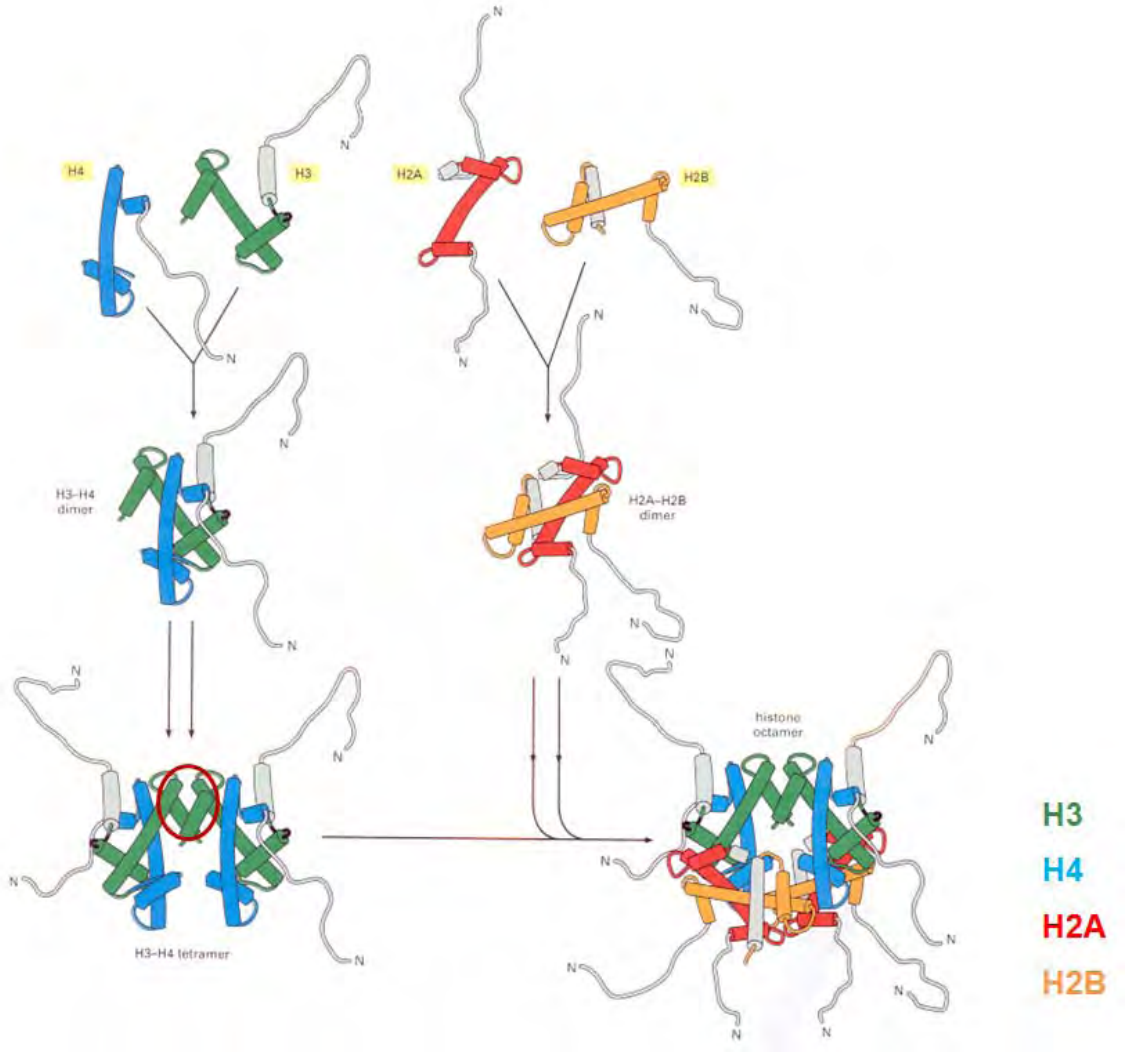

CHAPTER II Materials and Methods

Plasmid Constructions

Mutagenesis

C-terminal mutations of *HHT2,* one of the yeast genes encoding histone H3, were generated according to QuickChange™ Site-Directed Mutagenesis protocol (Stratagene), and were sequenced by OPK1173, which located 150bp upstream from *HHT2* ORF (Table 2.1, 3.1). In this method, two complementary primers that span the site to be mutated were used for PCR followed by DpnI digestion. The templates, which contain the wild-type *HHT2* gene, are derivatives of *ARS-CEN* plasmids pRS413 (*HIS3*), pRS414 (*TRP1*), pRS415 (*LEU2*) or pRS416 (*URA3*) (Sikorski and Hieter, 1989).

N-terminal Tagging

The plasmids containing Myc- or Flag-tagged *HHT2* were obtained from Rando lab (Dion et al., 2007). The insertion of the V5 tag at the 5'end of *HHT2* was generated by PCR using two phosphorylated primers (OPK1174, 1175) with half of V5 sequence at each 5'end respectively. The PCR reaction was gel purified after DpnI digestion, and the products were ligated O/N at 16^{o}C. The product was confirmed by sequencing. The insertion of the biotin receptor sequence at the 5'end of *HHT2* was generated using the same strategy with the primers of OPK1204, 1205.

Sub-cloning using restriction endonuclease sites such as NotI, XhoI and AgeI (NEB) were performed to generate mutant *hht2* alleles with different N-terminal tags (Myc, Flag or V5) and different selectable markers (*HIS3*, *TRP1, LEU2* or *URA3*).

BirA Integration

The fragment containing BirA open reading frame (encoding biotin-protein ligase) in pET28a vector (obtained from Eric Campeau) was excised by XbaI and BlpI, and inserted through Klenow treatment and blunt-end ligation into downstream of GPD (glyceraldehyde-3-phosphate dehydrogenase) promoter and upstream of PGK (3-phosphoglycerate kinase) terminator in integration vector pRH98-20, which was excised by SalI and BamHI. The product was sequenced by OPK1218, which located 80bp upstream from BirA gene. The constructed plasmid was cut within *URA3* by StuI, and integrated into the *ura3* locus of chromatin in target strains by transformation.

Tail Deletion

The *HHT2*-N truncation (1–28aa) was generated by 'Touchdown' PCR (Don et al., 1991) with 5'-phosphate primers (OPK1184, 1185) containing flanking sequences of N-terminal tail followed by ligation. The product was confirmed by sequencing.

TK Insertion

The NotI-KpnI cassette containing TK (thymidine kinase) gene was excised from p306-BrdU-Inc (Viggiani and Aparicio, 2006) and inserted into the NotI site of p44 (*hht2*-L110I, A111W, L131I) through Klenow treatment and blunt-end ligation.

Construction of libraries of *hht2* with randomized codons

p46 (*hht2*-L127V, L131V, *TRP1*) was used as the template to generate four libraries, each with randomized nucleotides at one of four H3 codons (110, 111, 127, 131). For each library, pairs of divergent 5'-phosphorylated primers were used with the randomized codon at the 5' end. Each PCR reaction includes 5 µl of 10x PfU Buffer (200 mM Tris-HCl pH 8.8, 100 mM $(NH_4)_2SO_4$, 100 mM KCl, 1%(v/v) Triton X-100, 1 mg/ml BSA), 1 µl of 10 mM dNTPs, 1 µl of each primer (OPK1206~1213, 10 µM), 1 µl of PfU polymerase, and sterile H_2O was added to a total volume of 50 µl. 100 ng of plasmid p46 was used as the template. Denaturation was done at 94^oC for 2 minutes initially and then 0.5 min for subsequent cycles. Annealing was carried at 60^oC for 0.5 min and the elongation was done at 72^oC for 7 minutes with 25 cycles of amplification. The entire sample was loaded onto 0.8% agarose gel for analysis. The full length PCR product was gel purified (10-16 ng/µl), and ligated overnight before transformation with 100 µl Top10F' competent cells. 1 ml LB was added after heat shock transformation and the cells recovered for 1.5 h at 37^oC. 100 µl cells were plated to check the colony number, and the rest of the transformation was put into culture tube with another 2 ml LB and antibiotic to

grow O/N before miniprep. The randomization of the desired codon in the four libraries of *hht2* was confirmed by sequencing (Figure 3.8A).

Yeast Strains

Strain PKY4171 [*MAT*a; Δ(*hht-hhf1*); Δ(*hht2-hhf2*); *leu2-3,112; ura3-62; trp1; his3; bar1::hisG*; p(*HHT1-HHF1, URA3, CEN*)] was used for tests of histone mutations, since the chromosomal genes encoding histones H3/H4 are absent. Low-copy plasmids containing mutated histone genes were introduced by LiOAc transformation, and then 5-FOA was used as a counterselecting agent (Boeke et al., 1987) to select against the *URA3* plasmid containing the wild-type *HHT1-HHF1* genes.

Strain PKY4487 [*MAT*a; Δ(*hht-hhf1*); Δ(*hht2-hhf2*); *leu2-3,112; ura3-62; trp1; his3; bar1::hisG*; p((*hht2*-L110I,A111W,L131I)-*HHF2*, *LEU2, CEN*); p((*hht2*-L127V,L131V)-*HHF2, TRP1, CEN*)] contained the two *hht2* alleles that were most studied in this work. Maintenance of the correct alleles was confirmed by PCR amplification of the *hht2-HHF2* locus and DNA sequencing.

Yeast growth and plasmid transformation of yeast cells were done according to standard yeast protocols (Rose et al., 1990).

MNase – ChIP - Western

Yeast Culture

110 ml cells (PKY4322) were grown in 4-amino acid dropout synthetic media (SD-Trp-Leu-Ura-His) with 200 rpm agitation at 30°C to an A_{600} of ~0.5. 37% formaldehyde was added to a 1% final concentration, and the cells were incubated for 15 minutes at 30°C with shaking at 200 rpm. 2.5 M glycine was added to a final concentration of 125 mM to quench the formaldehyde. The cells were spun down at 3500 rpm for 5 minutes at 4°C (all following steps were done at 4°C unless otherwise indicated) and were washed once with 50 ml of room temperature sterile MilliQ water.

Micrococcal Nuclease Digestion

The cell pellets were resuspended in 900 µl of NP+ buffer (250 mM spermidine, 4 mM β-ME, 10% NP-40, 50 mM NaCl, 10 mM Tris-Cl pH 7.4, 5 M $MgCl_2$, 1 mM $CaCl_2$). 18 µl protease inhibitor mix (final: 0.7 mg/l pepstatin, 5 mg/l leupeptin, 1 mg/l aprotinin, 3 mg/l E64, 1 mg/l benzamidine, 1.1 mg/l phosphoramidon and 1 µM chymostatin) and 10 µl PMSF (final: 1 mM) were added. The cells were resuspended completely and put into a screwcap tube containing 0.5 ml glass beads (BioSpec, 0.5 mm) before beating at a maximum speed for 1 minute in a beadbeater (BioSpec Mini-BeadBeater Model 8) for 3 times with 5 min intervals. The tube bottom was punctured with a red hot 26 gauge needle and spun for 2 min at 1500 rpm into a plastic tube. The lysates were resuspended completely and transferred to eppendorf tubes which contain micrococcal nuclease (Worthington Biochemical, 20 U/µl in Tris-Cl pH7.4), and were then incubated at 37°C for 20 minutes – the amount

of MNase used was determined in initial titrations to yield >80% mononucleosomal DNA (usually 20 µl), but to repeat these results an independent titration should be carried out as a preliminary study. The digestion was halted by shifting the reactions to 4°C and adding 0.5 M EDTA to a final concentration of 10 mM.

Nucleosome Immunoprecipitation

Buffer L (50 mM Hepes-KOH pH 7.5, 140 mM NaCl, 1 mM EDTA, 1% Triton X-100, 0.1% sodium deoxycholate), protease inhibitor mix (1x) and PMSF (1 mM) were assembled from concentrated stocks. The supernatant from the digested lysates was taken after spinning at 10,000g for 20 min and was incubated with 50% Sepharose Protein A Fast-Flow bead slurry (Sigma, 20 µl slurry for about 300 µl lysates, equilibrated in Buffer L with 0.1 mg/ml insulin O/N) for 1 h on a tube rotisserie rotator. The beads were pelleted with a 1 minute spin at 8,000g and the supernatant was taken to measure protein concentration by Bradford assay (usually 3-7 mg/ml, variable for each experiment and each strain). 20 µl of the supernatant was set aside as IP input material and 100 µl for test of MNase digestion. With the remainder, anti-V5 antibody (Invitrogen, 4µl per 2.1mg total protein), about 20 µl 50% Protein A bead slurry, protease inhibitor mix (1x) and PMSF (1 mM) were added to about 300 µl lysates and the tube was rotated overnight (~16 hours). The beads were pelleted by a 1 minute spin at 8,000g. After removal of the supernatant, the beads were washed twice with Buffer L in the following

manner: 1 ml of the buffer would be added, the sample was then rotated on the tube rotisserie for 5 minutes, and the beads would then be pelleted in a 30 second spin at 8,000g and the supernatant removed. After the last wash, 12-16 µl of 1.5x SDS sample buffer with 0.8 µl of β-ME was added to the beads following by boiling for 3 minutes. The beads were spun for 2 minutes at 10,000g, and the eluate was taken as IP sample.

DNA Extraction

After trial MNase digestions, DNA was extracted to determine the mononucleosome yield. 100 µl digested sample was incubated with 1.7 µl proteinase K (20 mg/ml) at 65°C for 3-4 hours, then 25 µl Stop Buffer (0.25 M EDTA, 5% SDS) was added. The sample was then extracted with an equal volume of Phenol : Chloroform : Isoamyl alcohol (25:24:1). Phase lock gel tubes (heavy, Eppendorf) were used to separate the phases, and 0.1 volume 3.0 M sodium acetate pH 5.2 and 1 volume of isopropanol were added to the supernatant. The DNA was pelleted by centrifugation at 14,000rpm for 10 minutes, washed once with cold 70% ethanol, and spun at 14,000rpm for 5 minutes at 4°C. After removing the supernatant, the pellets were allowed to dry and then were resuspended in 25 µl TE supplemented with NEBuffer 3 (100 mM NaCl, 50 mM Tris-HCl pH 7.9, 10 mM $MgCl_2$, 1 mM dithiothreitol) and 0.5 µg of RNase A. The samples were incubated at 37°C for one hour and then run with orange loading dye (6x, 0.4% orange G, 40% sucrose). Orange G migrates faster than 100bp DNA on a 2% agarose gel.

Western Blot Analysis

6-9 µl of Input sample and 4-9 µl of IP sample were loaded onto a 17% SDS-PAGE gel, transferred onto nitrocellulose membrane, and probed with mouse anti-V5 (Invitrogen, 1: 5,000), rat anti-Flag (Novus, 1: 500), mouse anti-c-myc 9E10 (Santa Cruz, 1: 1,000), or rabbit anti-H3 (Abcam, 1: 2,500). The secondary antibody used is horseradish peroxidase (HRP) conjugated donkey anti-mouse IgG (Jackson, 1: 10,000), donkey anti-rat IgG (Jackson, 1: 10,000) or goat anti-rabbit IgG (GE Healthcare, 1: 5,000). All primary and secondary antibodies were diluted in TBS with 0.1% Tween 20 and 5% milk. To quantify the signals from immunoblots, we detected the signals by chemiluminescence on a LAS-300 (Fujifilm) and measured the intensities using Image Gauge (Fujifilm). Then the IP percent number was calculated, which is the ratio of the recovered signal from IP sample to original signal from Input sample in the same amount of cell lysates.

Genetic Screen

Yeast Colony PCR

Each PCR reaction includes 2 µl of 10x Colony PCR Buffer (0.125 M Tris-HCl pH 8.5, 0.5625 M KCl), 1.2 µl of 25 mM $MgCl_2$, 0.4 µl of 10 mM dNTPs, 1µl of each primer (OPK1219/1221 or OPK1219/1222, 10 µM), 0.4 µl of Taq : PfU (16:1) polymerase, and sterile H_2O was added to a total volume of 20 µl. A small amount of cells (about 0.25 µl worth) were picked from a colony using a

yellow pipet tip and swirled into PCR tubes as the template. Denaturation was done at 94^{o}C for 8 minutes initially and then 1 min for subsequent cycles. Annealing was carried at 60^{o}C for 1 min and the elongation was done at 72^{o}C for 2-4 minutes with 35 cycles of amplification. The entire sample was loaded onto a 0.8% agarose gel for analysis and gel purified for sub-cloning.

Table 2.1 Primers used in this study.

OPK1173	GCGTGATAACAGCGTGTTGTGCTCTCTCGC
OPK1174	Phos - CTCCTCGGTCTCGATTCTACGGGAGCCAGAACTAAACAAACAGCTAGA
OPK1175	Phos - AGGGTTAGGGATAGGCTTACCTTCCATTGTGGAGTGTTTGCTTGGATC
OPK1184	Phos - CATTGTGGAGTGTTTGCTTGGATCC
OPK1185	Phos - GCCCCATCTACCGGTGGTGT
OPK1204	Phos - AAAATCGAGTGGCATGAAGGAGGCGCCAGAACTAAACAAACAGCTAGA
OPK1205	Phos - CTGGGCTTCAAAAATATCATTCAGGCCCATTGTGGAGTGTTTGCTTGG
OPK1206	Phos - NGCTGCTATTCACGCTAAG
OPK1207	Phos - NNATTAGTGTCTTCAAACAAAGAG
OPK1208	Phos - NGCTATTCACGCTAAGCGT
OPK1209	Phos - NNCAGATTAGTGTCTTCAAACAA
OPK1210	Phos - NNGCCAGAAGAGTTAGAGGT
OPK1211	Phos - NTTTGATATCCTTCTTTTGGATAGTAA
OPK1222	Phos - NNAGAGGTGAAAGATCATGA
OPK1213	Phos - NTCTTCTGGCAACTTTGATAT
OPK1218	TCCCGCACGGCGCCGCATTGGCGGCATTGTTCAGTG
OPK1219	ACGGCTATGGCTCGGTGTCAAAAC
OPK1221	CGGTGGCGGCCGCTCTAG
OPK1222	AACTTTAGCCACGTCGTTGGGGAG

CHAPTER III Results

Protein Design

How can we generate the obligate heterodimeric H3 mutant to break nucleosomal symmetry? As stated before, the four-helix bundle on the H3-H3 C-terminal interface is important for holding together the two halves of the H3/H4 tetramer scaffold, and this interface is maintained by hydrogen bonds and several hydrophobic bonds formed by leucine and alanine (Figure 3.1A). By computational protein design (Bolon et al., 2005), specific residues at the H3-H3 interface were targeted to generate H3 heterodimeric pairs designed via a “bump and hole” approach, with clashes or voids in the hydrophobic core to favor heterodimeric interactions while disfavoring homodimerization. Dr. Bolon designed six sets of H3 mutations (Table 3.1; Figure 3.1B). As shown in the table, pairs of H3 variants with mutations listed in columns A and B were predicted to form heterodimers. The first set has two similar designs for the “A” half of the pair, so the corresponding plasmids and H3 mutants were termed 1A and 1a. In five sets (No. 1-4), the targeted residues formed hydrophobic bonds in the H3-H3 interface, while in the last set (No. 6), the buried hydrogen bonds were replaced with hydrophobic interactions.

Figure 3.1 Designed obligate heterodimeric H3 mutants. A) The four-helix bundle on H3-H3 C-terminal interface within H3/H4 tetramer. This interface contains several hydrophobic bonds formed by leucine and alanine molecules as shown by the ball-and-stick models. B) By computational protein design, specific residues at the H3-H3 interface were mutated to L127V, L131V (yellow) and L110I, A111W, L131I (green), which are ‘1a’ and ‘1B’ in Table 3.1, so that they could form a bump-hole interface to increase interaction affinity. C, D) Each single H3 mutant shouldn't interact with itself due to clashes or voids in the hydrophobic core.

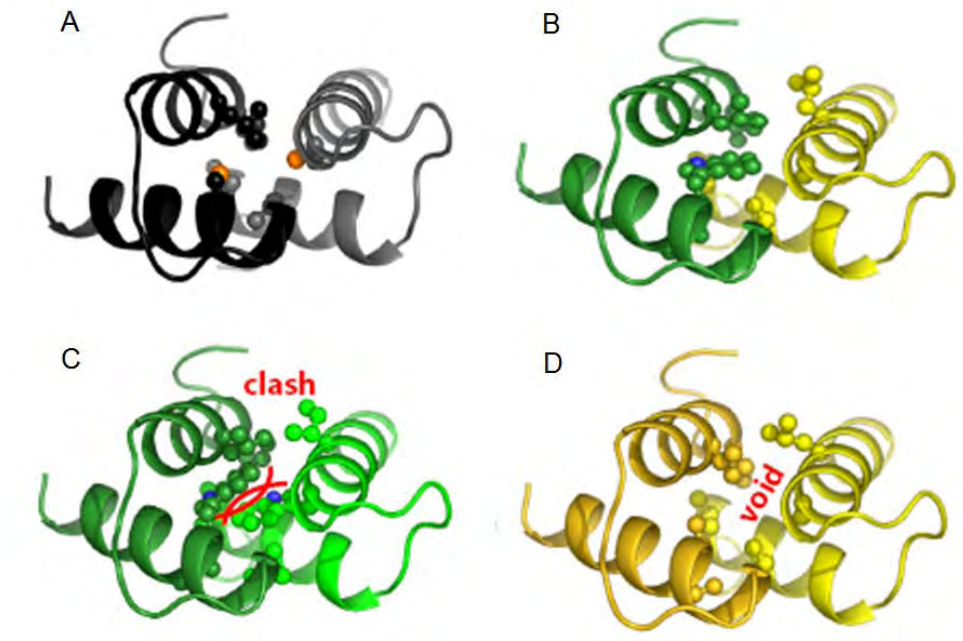

Table 3.1 Designed sets of H3 C terminal mutations on H3-H3 interface using computational method. H3 with mutations in column A and B of each set are designed to form a heterodimer, in which asymmetric mutations pack efficiently, while self-pairing lead to van der Waals clashes or voids in the hydrophobic core. The first set has two similar designs for A, so the corresponding plasmids and H3 mutant are called 1A and 1a. No.5 was designed for other purposes so it is not shown here.

Design #	A	B
1	L127V, L131G	L110I, A111W, L131I
	L127V, L131V (1a)	
2	A111S, L127V	L110I, A111G, L127F, L131I
3	A111N, L131I	A111C, L127N, L131I
4	A111N, L131V	A111M, L127A, L131Q
6	H114M	A115V, R117S, D124M

Genetic Test

Histones along with their modifications are highly conserved in eukaryotic species. Our experiments were performed using the budding yeast *Saccharomyces cerevisiae*, in which precise control of the cell cycle synchrony and the expression of histone genes is allowed, and the most comprehensive analyses of histone modifications have been carried out (Millar and Grunstein, 2006).

A series of yeast shuttle vectors (pRS) were used to carry H3 mutant genes. These pRS vectors are mitotically stable with a yeast centromere sequence (*CEN*) and an autonomously replicating sequence (*ARS*), and differ only in the yeast selectable marker genes (*HIS3, TRPl, LEU2 and URA3*) (Sikorski and Hieter, 1989) (Figure 3.2A). Mutant H3 and wild type H4 genes are under control of the natural divergent promoter from the *HHT2-HHF2* locus for simultaneous expression. The N-terminus of H3 has an epitope tag such as V5, Myc or Flag for co-immunoprecipitation experiments, and the C-terminus has the designed mutations to form altered H3-H3 interface (Table 3.1).

The yeast strain (PKY4171) that served as the host for all of these plasmids contains auxotrophic mutations, and both endogenous H3-H4 gene pairs were deleted. The only copy of H3-H4 genes resides on a plasmid containing the *URA3* marker gene, which can be selected against by 5-Fluoroorotic acid (5-FOA) due to conversion of 5-FOA into a toxin by the *URA3* gene product

(Boeke et al., 1987). In this way, cells carrying H3 mutant combinations were tested for viability in the absence of wild type H3, and strains with various H3s were generated (Figure 3.2 B).

As shown in Figure 3.3C, three heterodimer designs – 1aB, 1AB, 2AB -- passed the initial genetic tests, and the growth of cells with '1AB' H3 mutants was much slower than the other two in the absence of wild-type H3. However, after very long incubation, growth of cells with 1a or 2A alone was found, with faster growth observed for '2A'. Design numbers 3 and 4 failed because a single half of the pair (3A or 4A) was sufficient to sustain growth in all three patches (Figure 3.3B). The cells with No.6 H3 mutant(s) (either single or pair) were inviable. From these results we know that the computational strategy in the first and second sets of mutations is the best one for heterodimer simulation.

For 1aB, 1AB and 2AB candidates, we did another genetic test. They were grown on YPD plates without selection, and then single colonies were picked and patched onto selective SD plates to see if any plasmid can be lost naturally. We found the loss of 1B plasmid in the '1AB' strain (4 colonies out of 24) but not the other two. However, in another more stringent test later, '1aB' was grown in liquid YPD media overnight before streaked on YPD plates, a very small percent of tiny colonies (about 5%) were found, which actually lost 1B plasmid. This is consistent with the fact that '1a' can survive by itself.

Since the cells with ‘1AB’ H3 mutants grew too slowly and lost plasmid in the absence of selection, and ‘2A’ grew faster than ‘1a’, we chose ‘1aB’ as the best heterodimer candidate for the following experiments.

Figure 3.2 The scheme of plasmid construction and strain generation. A) Yeast shuttle vectors (pRS) with CEN, ARS and selectable marker genes were used to carry *hht2-HHF2* genes. HHT2 was tagged at the N terminus and mutated at the C terminus. B) The plasmids with *hht2* were transformed into the yeast strain with HHT2-HHF2 on a plasmid containing *URA3*, and then plated on FOA media (w/ amino acids drop out) to generate viable strains with H3 mutant combinations.

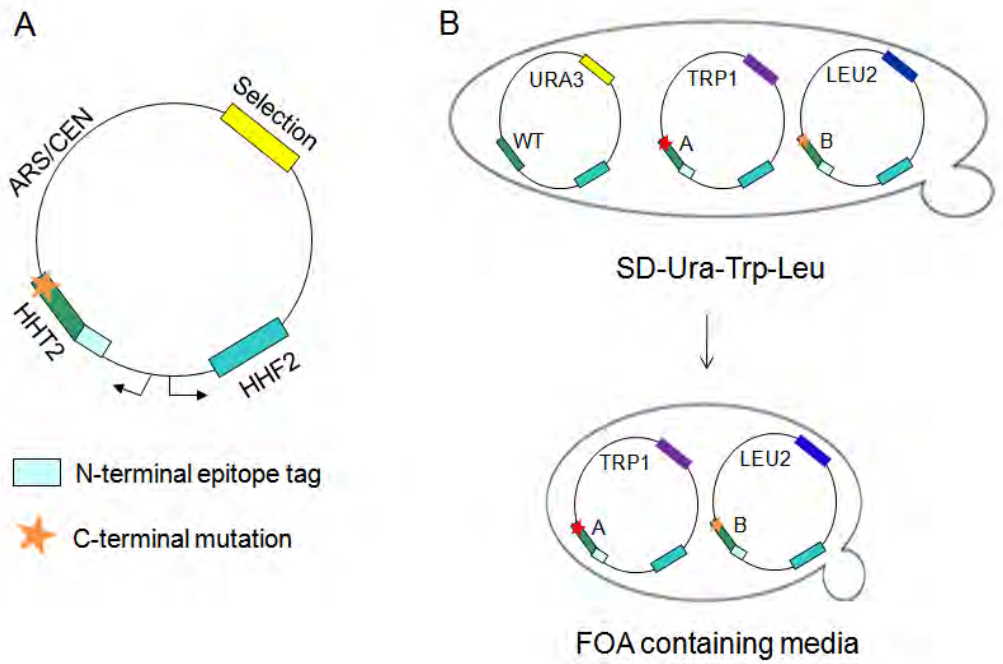

Figure 3.3 Test of viability of strains with designed H3 mutants. Three independent isolates of yeast strains carrying the indicated *HHT2* alleles were patched on FOA media. Plates were grown at 30°C and photos were taken at different time points as indicated by “D” for days. A) The *ARS-CEN, TRP1* plasmid pRS414 (vector) and a pRS414 derivative containing the wild-type *HHT2* gene (wt) were transformed into PKY4171 and plated on FOA media as negative and positive controls, respectively. B) Heterodimer designs #3 and 4 failed because a single H3 mutant (3A or 4A) was sufficient to sustain growth in all three patches. All combinations of design #6 H3 mutant(s) (either single or paired) were inviable. C) The cells with 1aB, 2AB H3 mutant pairs survived and grew rapidly on FOA media, and the growth of 1AB was slower. Growth of cells with 1a or 2A alone was found after long incubation, and ‘2A’ grew faster.

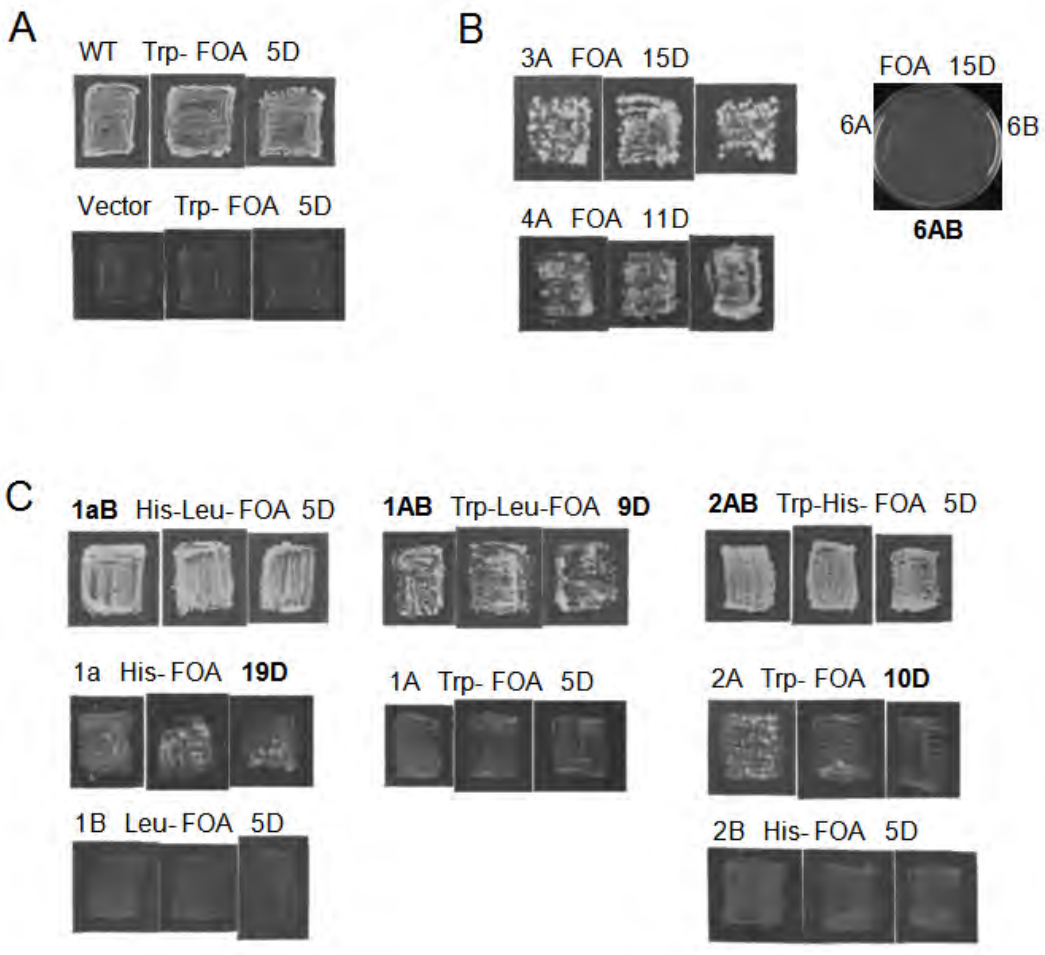

Biochemical Test

The candidate (1aB) provided by genetic tests needed to be further verified biochemically to determine whether the designed heterodimeric H3s exist in a 1:1 ratio *in vivo*. We tested this by co-immunoprecipitation analysis of digested chromatin.

Since the strain with '1a' alone could sustain slow growth, it is a question whether *in vivo* '1a' only co-precipitates with '1B', but not with itself. We generated the strain with V5-tagged and Flag-tagged '1a', and two copies of Myc-tagged '1B' to balance the expression of 'a' and 'B' (Figure 3.4A). In order to generate >80% mononucleosomes, we titrated the amount of Micrococcal Nuclease (MNase) to use for digestion and found that 2.1 µl MNase per 100 µl cell lysates (37^{o}C, 20 min) was sufficient. Increasing the incubation time would result in digestion of the DNA wrapped around the core histones. And we also titrated the amount of anti-V5 antibody to use for immunoprecipitation and found that 4 µl antibody (25 ng/µl) per 2.1 mg total protein in the cell lysates could almost deplete the V5-tagged H3. As shown in Figure 3.4A, while Myc-'1B' was pulled down with V5-'1a' (2%), a comparable amount of Flag-'1a' was also pulled down (0.8%). And the percent IP number of V5-tagged H3 (13.7%) was much bigger than the other two, suggesting that there could be some V5-'1a' self-interaction or the presence of H3/H4 dimers in the cell lysates. Anti-Flag IP was also performed in the same strain. The

signal of V5-‘1a’ was detected in the IP sample (0.5%) while 1.5% Myc-‘1B’ were pulled down. Together, these data suggested that the H3 pair ‘1aB’ was frequently, but not exclusively heterodimeric *in vivo*.

To rule out the possibility that mononucleosomes might be crosslinked together in trans and produce artificial co-immunoprecipitation signals, two strains separately carrying V5-tagged and Flag-tagged ‘1a’ were generated and analyzed as a negative control (Figure 3.4B). The strains were grown separately and then mixed prior to crosslinking. Nuclei were then prepared and digested by MNase as usual, and the resulting nucleosomes were precipitated with the anti-V5 antibody. Unlike the previous experiment, there was hardly any signal of Flag-‘1a’ found in the IP sample. For the above IPs, DNA was extracted from the Input samples and the ratio of dinucleosomes to mononucleosomes was about 2%. So most digested chromatin should exist as uncrosslinked mononucleosomes in the cell lysates.

Since the strain with ‘1B’ alone was inviable in the genetic test, we tried to confirm this in the IP experiment. A strain carrying one copy of each V5-‘1B’, Flag-‘1B’ and Myc-‘1a’ was generated and anti-V5 IP was performed (Figure 3.4D). There was little visible signal of Flag-‘1B’ in the IP sample, and the percent IP numbers of V5-‘1B’ (3.3%) and Myc-‘1B’ (2.5%) were close, suggesting that ‘1B’ seldom or never interact with itself *in vivo*. So the result of IP experiment for ‘1B’ is consistent with the genetic test.

As indicated in the above experiments, there is probably a certain amount of ‘1a’ self-interaction *in vivo*. We tried to increase the proportion of 1a-1B heterodimer by overexpressing ‘1B’ in a 2μ plasmid. Although we didn’t quantify the degree of ‘1B’ over-expression, the IP percent numbers showed that it didn’t help – for anti-V5 IP: 9% V5 1a, 3.8% Flag 1a, 4.1% Myc 1B; for anti-Flag IP: 10% Flag 1a, 2.1% V5 1a, 3.9% Myc 1B.

The IP experiments have some limitations, for example, anti-Flag antibody was not efficient in detection and strong background signals existed in the anti-Flag IP samples; Even a large amount of MNase was not able to produce 100% mononucleosomes without dinucleosomes. So we are constructing another system to test self-interaction of H3 mutant. By the use of biotin receptor sequence (bio-) and biotin-protein ligase (BirA), H3 heterodimer with one biotinylated partner and one untagged can be generated. After we get purified mononucleosomes through Sucrose Gradient, the different combinations of the two partners could be separated either by gel shifting (with the help of streptavidin) or electronic microscopy (with gold labeling). Now we have already generated the strains with ‘bio-1a’ or ‘bio-1B’, and tested the biotinylation of histones with expression of BirA (Figure 3.5).

Figure 3.4 ‘1a’ co-precipitates with itself while ‘1B’ does not. A) Yeast strain carrying the indicated *HHT2* alleles was digested by MNase and precipitated by anti-V5 antibody. The proper amount of anti-V5 antibody to use was determined by titration and the percent IP numbers were calculated by quantifying the signals in the rightmost lane. B) Two strains carrying the indicated *HHT2* alleles were grown separately and then mixed and digested by MNase and precipitated by anti-V5 antibody. C) For both the above IPs, DNA was extracted from the Input samples and run on the 2% gel next to 100bp DNA marker. The arrow indicates the length of mono-nucleosomes. D) Yeast strain carrying the indicated *HHT2* alleles was digested by MNase and precipitated by anti-V5 antibody.

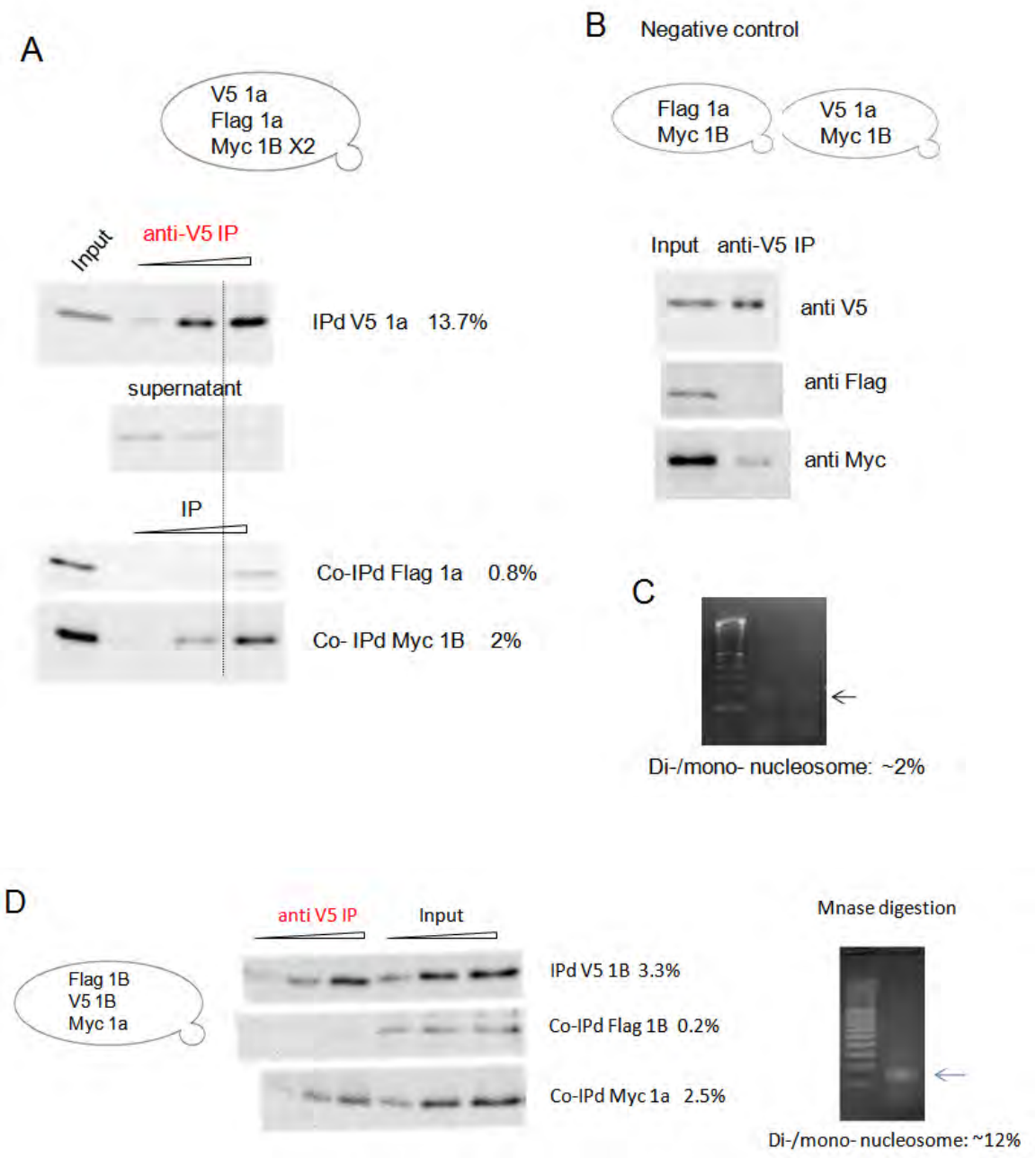

Figure 3.5 Biotinylation of H3 with expression of BirA. A) Four strains with the indicated *HHT2* alleles were generated, of which two strains had BirA integrated into the chromosome and the other two didn't. Whole-cell alkaline lysis extracts of the strains grown in SD media were analyzed by probing with HRP-linked streptavidin, since biotin binds very tightly to streptavidin with a dissociation constant K_d in the order of 10^{-15}. The arrow indicated the biotinylated H3 with the expression of BirA. B) The blot was stripped and reprobed with anti-H3 antibody. The biotin receptor tagged H3 was shown by the arrow.

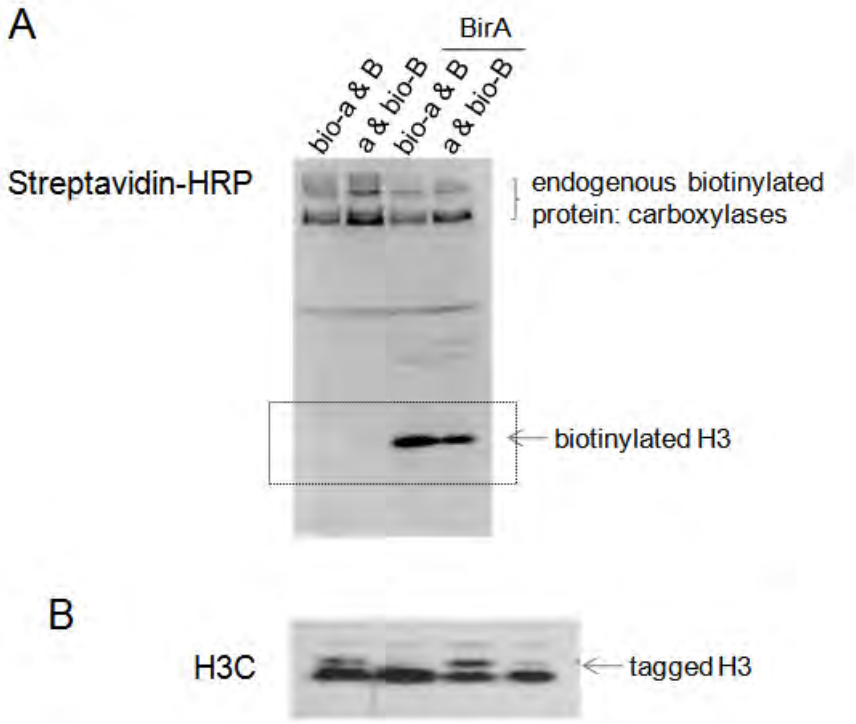

Microarray

It has been reported that the amino termini of H3/H4 have redundant functions in regard to viability and nucleosome assembly (Ling et al., 1996). The H3/H4 N-termini are also required for silencing of the subtelomeric genes and the HM mating loci (Thompson et al., 1994). Both H3 N-terminal (residues 4-15) deletions and acetylation site substitutions (Lys9, 14, 18) hyperactivate *GAL1* promoter (Mann and Grunstein, 1992). From a versatile library of 486 H3/H4 mutants generated in *S. cerevisiae,* it was found that most H3 N-tail deletions are defective in the nonhomologous end joining (NHEJ) repair and rDNA silencing (Dai et al., 2008). Sabet and his colleagues found in yeast that the absence of H3 tails (1-28) constitutively activates *CHA1* promoter and causes chromatin remodeling at the promoter site (Sabet et al., 2003). Besides, they conducted microarray analysis to test the gene transcription in the H3 tailless strain. Among 6800 genes tested, less than 500 genes were found to be affected by H3 tail deletion. 366 genes increased in expression and only 101 decreased ($P < 0.05$). However, there is no “substantial overrepresentation of any one class of gene (e.g., transcription factors, cell-cycle components, DNA repair, etc.)”.

The idea of “single-tailed H3” has only been tested *in vitro* very recently (Li and Shogren-Knaak, 2008). They mixed the His_6-tagged full-length H3 with an excess amount of N-terminally-truncated H3 and other core histones, and

enriched the tagged nucleosomes by affinity purification. In this way they collect a considerable amount of histone octamers with asymmetrical H3 tails, and found that cooperative acetylation mediated by SAGA (Spt-Ada-Gcn5-acetyltransferase) complex requires the presence of both H3 tails. This study gives us a clue that single-tailed H3 nucleosomes may not be as fully functional as intact ones.

Although ‘1aB’ is imperfect as a heterodimer, there should still be a considerable amount of heterodimeric H3 in the nucleosomes of the strain carrying these two H3 mutants. So we generated four strains with single-tailed or tailless ‘1aB’ to test the role of histone H3 tail symmetry on gene expression *in vivo* (Figure 3.6). One strain expresses full-length ‘1a’ and ‘1B’ (intact), one expresses N-terminally truncated ‘1a’ and ‘1B’ (tailless), and another two express either tailless ‘1a’ with intact ‘1B’ or tailless ‘1B’ with intact ‘1a’ (single-tailed). The strain carrying intact heterodimeric H3 serves as control for effects of altered H3 interface. The expression levels of ‘1a’ were found to be higher than that of ‘1B’ from the western blot of single-tailed strains (Figure 3.6C), which indicates that ‘1a’ probably accounts for a bigger percent of the total H3 in the nucleosomes.

The preliminary expression assay was done by Jeremy Shea from Rando lab (Figure 3.7). While 1aB interaction surface alone causes lots of gene expression changes, a small subset of genes were differentially regulated by having 1 tail, and in some cases it mattered whether it was on a or B. In the

single-tailed strain, one set of genes showed similar expression level to the intact strain, which indicates that the two copies of H3 tail function redundantly for these genes. Another set of genes showed similar patterns to the tailless strain, which means that both copies of H3 tail/modifications (nucleosomal symmetry) are required for full expression regulation of these genes.

Figure 3.6 Strains carrying tail-mutant ‘1a’ and/or ‘1B’. A) A schematic of the strains containing intact, single-tailed and tailless H3 heterodimer. B) The strains with intact, single-tailed and tailless ‘1aB’ were generated and plated on SD-Trp-Leu for 6 days before the picture was taken. C) Whole-cell alkaline lysis extracts of the strains with indicated *HHT2* alleles were analyzed by immunoblotting with anti-H3 antibody. The upper bands are the full-length H3 and the lower bands are N-terminally (1-28) truncated H3.

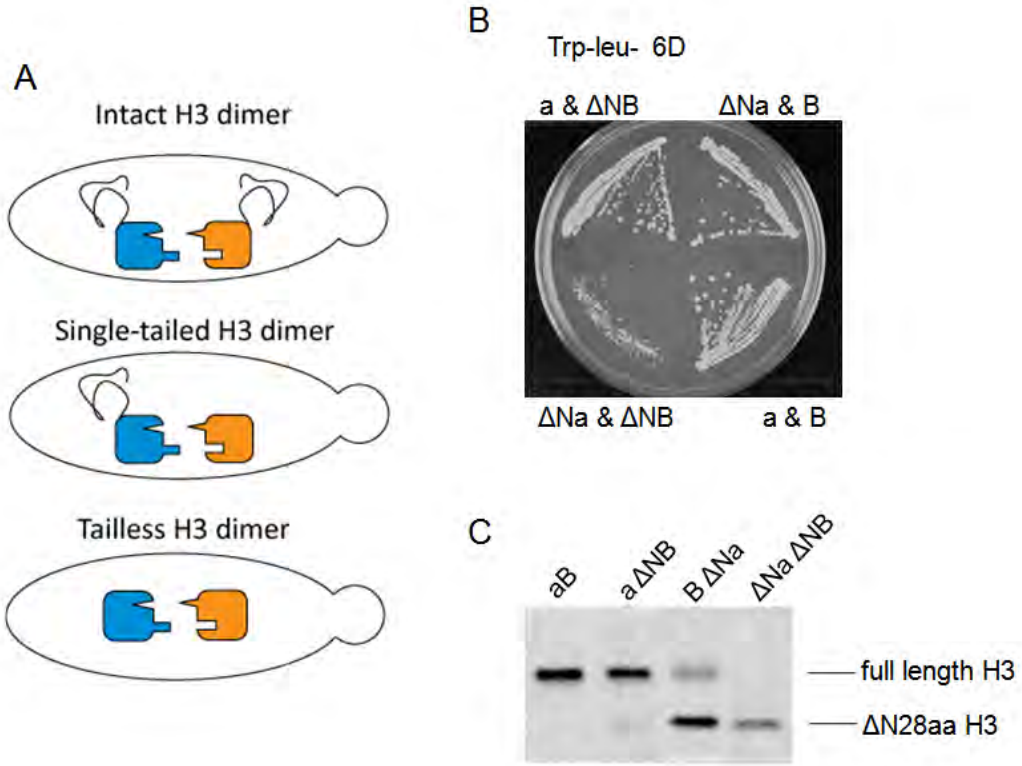

Figure 3.7 Gene expression in tail mutants and control strains. Six strains were grown and the mRNA was extracted for microarray analysis. The schematic above the array shows the H3 combinations: orange circles mean wildtype H3/H3 interface and green circles represent the asymmetric a/B interfaces. The columns from left to right represent: WT vs. tailless; WT vs. ‘aB’; ‘aB’ vs. two single-tailed ‘aB’; ‘aB’ vs. tailless ‘aB’. All genes are shown in the left panel with the top and bottom being genes that change over 0.6 in the column of ‘aB’ vs. tailless ‘aB’, and these genes are zoom up and then sorted by the amount they change in the single-tailed mutant. Genes that show similar expression between single-tailed and intact/tailless are crudely annotated.

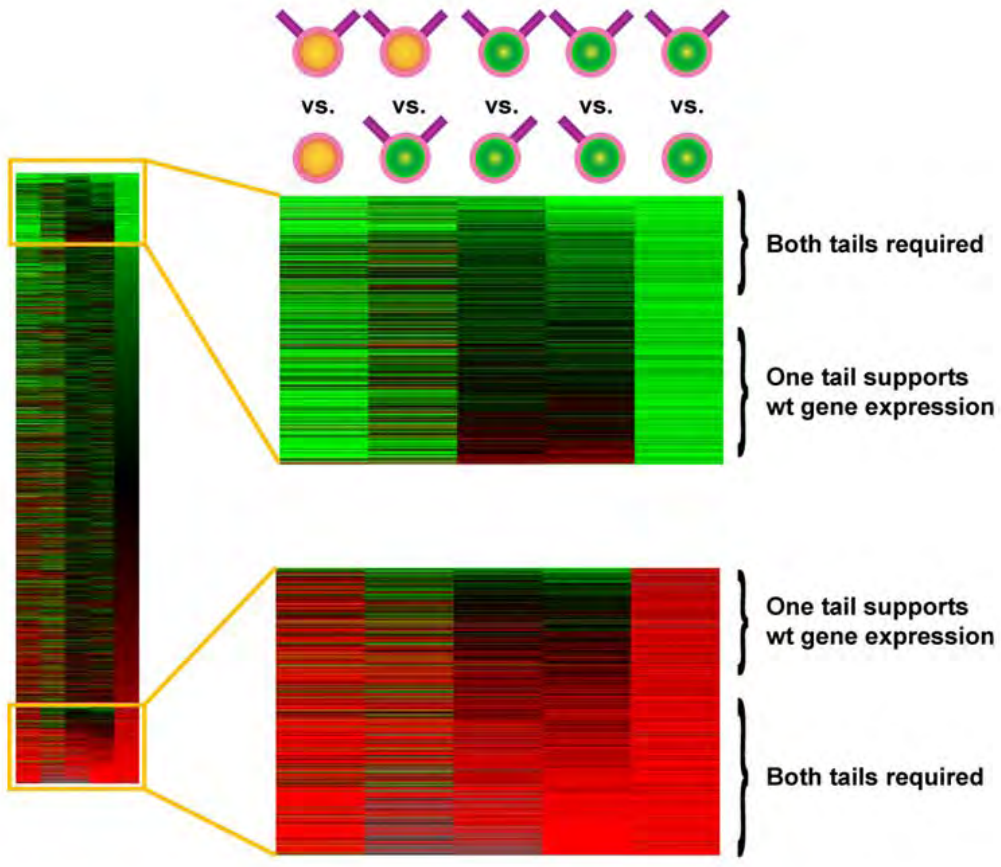

Genetic Screen

Since ‘1aB’ is an imperfect heterodimer due to ‘1a’ self-interaction, we attempted to generate more stringent heterodimer by making minor mutations on ‘1a’ (*hht2*-L127V, L131V). Because there are a total of four different sites of H3 C-terminus that were mutated on ‘1aB’ interface - 110, 111, 127 and 131, we tried to randomly mutagenize each of these four residues respectively in ‘1a’, thus generate four libraries to screen for better ‘a*’. The trace data for sequencing of the four mutagenized sites are shown in the Figure 3.8A. Although there were preferences for certain nucleotides at some sites, the mutagenized codons are generally random.

We have two strategies for screening. The first one takes advantage of FUdR (5-fluoro-2’-deoxyuridine) and *TK* (thymidine kinase) gene. It is known that the presence of TK causes sensitivity to the thymidine analogue FUdR. So if *TK* is introduced into the plasmid expressing ‘1B’, this plasmid could be selected against on plates containing FUdR. The amount of FUdR to use was titrated and the concentration of 40 μg/ml was found to be sufficient. As shown in Figure 3.8B, we firstly screened for viable ‘a*B’ on FOA plates and then screened for inviable ‘a*’ on FUdR plates. The candidates were picked up from FOA plates (Figure 3.8C), colony-purified on FOA and SD-Trp-Leu plates in sequence, and then patched on SD-Trp-Leu as master stocks, which were confirmed on SD-Trp+FUdR plates as well (Figure 3.8D). We screened about 1000 transformants for the library of ‘127’ by replicating, and then

screened 100 transformants for each of the other three libraries (110, 111, 131) by streaking individual colonies (Figure 3.8C). However, most of the initial candidates developed FUdR resistance during colony purification. We did colony-PCR to amplify the *hht2* and *HHF2* loci of 6 candidates, and the sequencing of PCR products showed original '1a', or mutant '1B', or *TK* gene deletion. Only three candidates showed mutant '1a' and original '1B' (Figure 3.8D). The mutations on '1a' are: 131-GGG (glycine), 131-GGT (glycine), 131-AAC (asparagine). We have constructed the strains expressing 'a*(131G)' or 'a*(131N)' and found that they are inviable in the absence of wild type H3, but viable in the presence of '1B (w/o TK)'. The new 'a*B' strains were streaked on YPD plates and then single colonies were picked and patched on SD-Trp and SD-Leu plates. No natural loss of either plasmid was found. So the new 'a*B' combinations are probably better than original 'aB' as a heterodimer.

From the above screen, we realized that *TK* gene containing plasmids were not stable under the selection pressure of FUdR -- *TK* deletion or recombination would probably occur. So we tried the second strategy as shown in Figure 3.8E. The four libraries of *hht2* (*TRP1*) with randomized codons were separately transformed into PKY4171 carrying the plasmid-borne wild type H3 (*URA3*). 153 transformants were picked for each library and streaked individually onto both SD-Trp-Ura and FOA plates at the same time. After incubation at 30^{o}C for 10 days on FOA, some 'a*' were found inviable in the absence of wild type H3 (Table 3.2A). The corresponding

transformants carrying inviable a* and WT from each library were then collected by picking a small amount of cells into a 25 ml of SD media. The mixed cells were grown to an A_{600} of ~0.5 but no more than 0.8. One tenth of the cells for each library were transformed with '1B' plasmid (*LEU2*) and plated on SD-Trp-Leu. All transformants were then put onto FOA by replica-plating. There were multiple colonies carrying viable 'a*B' coming out for each library (Table 3.2A), and the specific mutations on *hht2* locus were determined by colony PCR and sequencing (Table 3.2B). This is a small-scale screen, out of which only some but not all codons of an amino acid were recovered. And there were contamination or background issues, leading to recovery of input codons and/or amino acids. However, from both genetic screens, we found that Glycine was preferred as a replacement of Valine at position 131. So 'a*(131G)' would probably disfavor homodimerization while 'a*B' is viable. 'a*(131G)' will be tested for self-interaction by IP experiments as described previously.

Figure 3.8 Genetic screens for better H3 heterodimers. A) Trace data of the sequencing for four a* libraries with randomly mutagenized codons on plasmid ‘1a’ (*hht2*-L127V, L131V, *TRP1*). B) The schematic of screening strategy. The transformants carrying the indicated *HHT2* alleles were patched on FOA plates to evict wild type H3. The strains viable on FOA were plated on FUdR media to evict ‘1B’ plasmid, which contains the *TK* gene. The strains that were inviable on FUdR were picked and colony-purified on FOA and SD plates. C) The transformants carrying the library of ‘a* (*hht2*-V131X)’ were patched on the FOA plate one by one. Then the cells were picked from FOA plates and patched on SD w/ FUdR. The strains carrying orginal ‘1a’ and ‘1B’ w/ or w/o *TK* gene served as negative controls. The red circles indicate the candidates. D) From the screen described above, three candidates of H3 heterodimer were shown with indicated mutations on ‘a*’. The cells were grown on the plates at 30^{o}C for 6 days before the pictures were taken. E) The schematic of the second screening strategy. The transformants carrying the indicated *HHT2* alleles were patched on FOA plates. Those strains that couldn’t survive on ‘a*’ alone were transformed with ‘1B’, and then were plated on FOA again to select viable ‘a*B’ combinations.

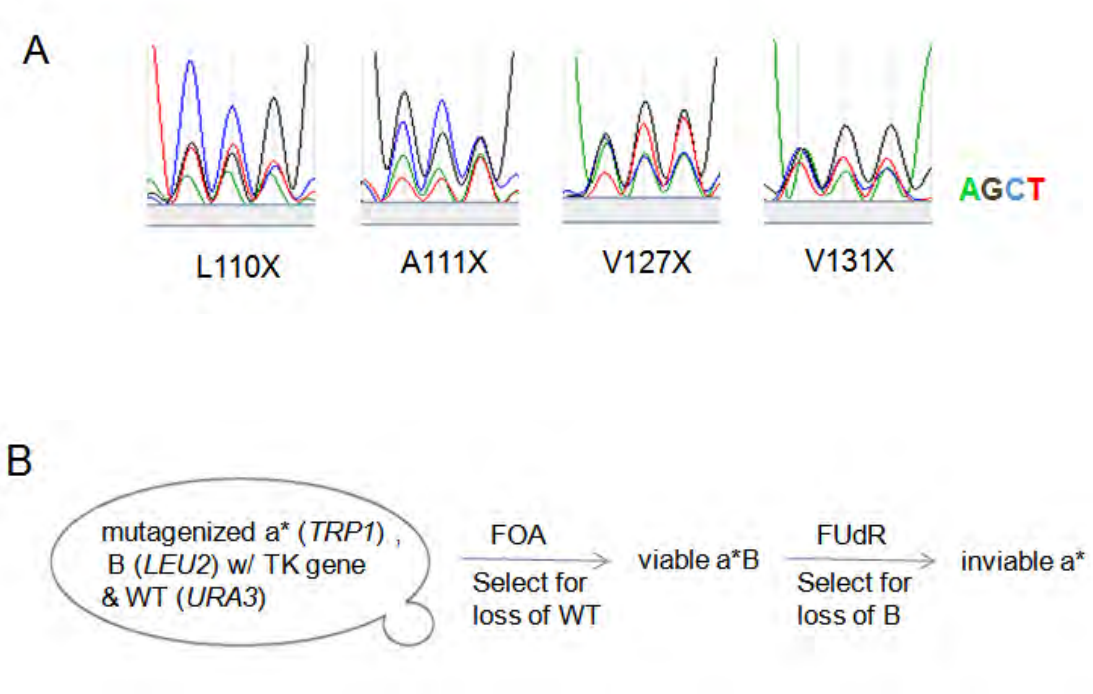

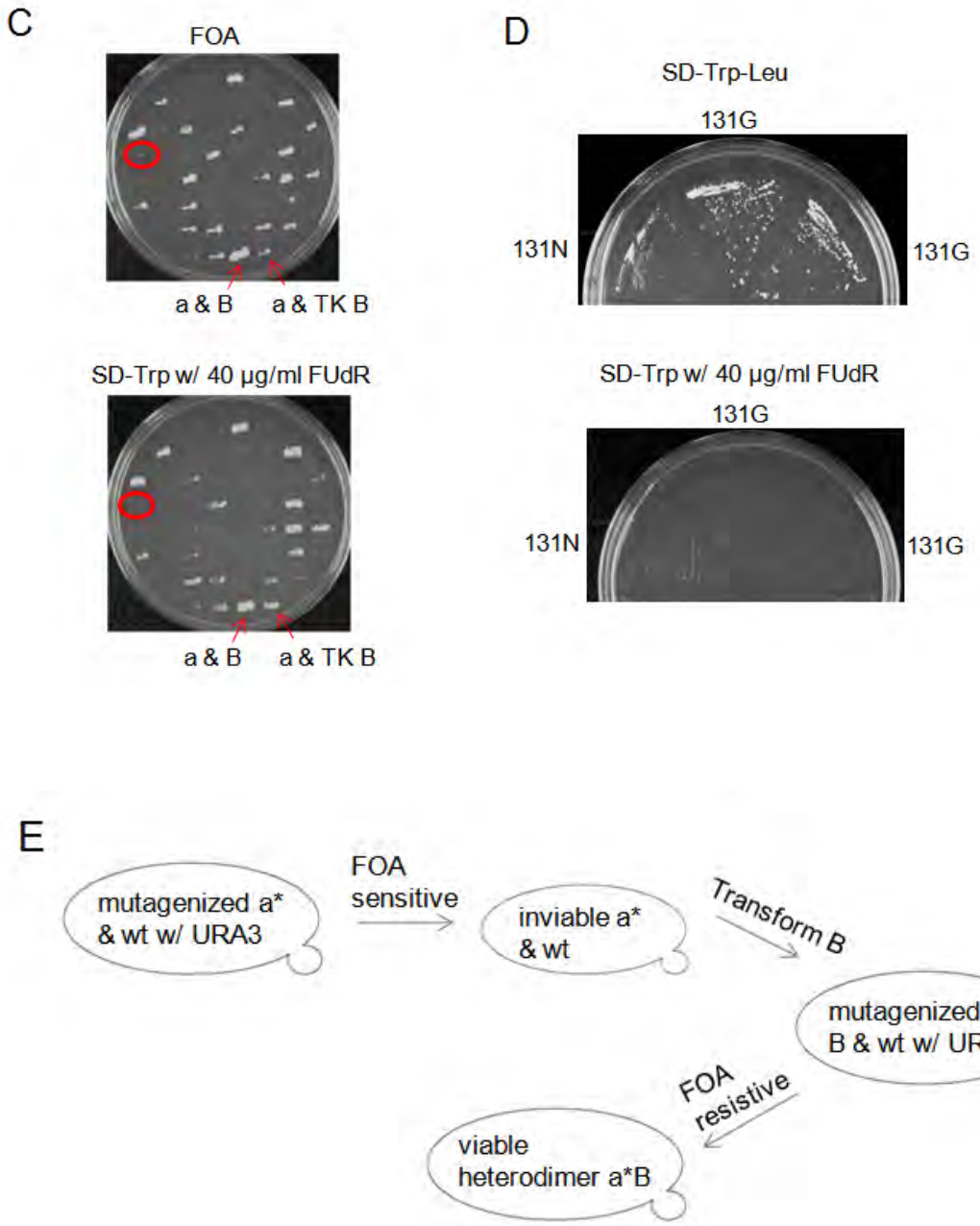
C
FOA
a & B
a & TK B
SD-Trp w/ 40 µg/ml FUdR
a & B
a & TK B
D
SD-Trp-Leu
131G
131N
131G
SD-Trp w/ 40 µg/ml FUdR
131G
131N
131G
E
mutagenized a* & wt w/ URA3
FOA sensitive
inviable a* & wt
Transform B
mutagenized a*, B & wt w/ URA3
FOA resistive
viable heterodimer a*B

Table 3.2 The statistics of the second genetic screen (Figure 3.8E). A) 'a*' represents the libraries carrying *hht2* alleles generated by random mutagenesis of a certain codon using 'a' (*hht2*-L127V, L131V) as the template. 'a**' represents 'a*' that couldn't sustain growth in the absence of wild type H3. 'a***' represents 'a**' that sustain growth in the presence of '1B'. B) The statistics of the sequencing results.

A

	Picked total transformants a* & wt	FOA sensitive transformants a** & wt	FOA resistive Transformants a*** & 1B
L110X	153	135	15
A111X	153	120	15
V127X	153	116	40
V131X	153	130	40

B

Codon	seq.	# isolates	Amino Acid	aa total
L110	ctg (input)	4	L	4
	cag	2	Q	4
	caa	2	Q	
	ttt	2	F	2
	atg	1	M	1
	cat	1	H	1
A111	gct (input)	2	A	7
	gcg	3	A	
	gcc	2	A	
	ggc	2	G	4
	ggt	1	G	
	ggg	1	G	
	tcg	3	S	4
	agc	1	S	
V127	gtt (input)	12	V	12
	gcg	10	A	12
	gcc	2	A	
	cat	4	H	4
	tat	1	Y	1
V131	gtt (input)	0	V	1
	gtg	1	V	
	tca	2	S	9
	tcc	5	S	
	tct	2	S	
	ggg	5	G	7
	ggc	1	G	
	ggt	1	G	
	gct	3	A	5
	gcc	1	A	
	gcg	1	A	
	act	4	T	5
	acc	1	T	
	cag	4	Q	4
	C +9aa	4		4
	tgc	2	C	2
	cat	2	H	2

CHAPTER IV Future Plans and Discussion

The data suggested that the best computationally-derived H3 pair was *frequently*, but not exclusively heterodimeric *in vivo*. In order to obtain a more stringent H3 heterodimer, random mutagenesis was performed on four codons in the original computational design, and then genetic screening of the mutant libraries was performed. For the candidates out of genetic screen, biochemical experiments will be performed to determine whether the altered H3 molecules are incorporated into nucleosomes with the expected stoichiometries of interaction. If more than one candidate were obtained, the best one should have similar growth rate and least expression change comparing to wild type.

For the new heterodimer, strains carrying the single-tailed and tailless H3s will be generated as done previously. Gene expression and nucleosome positioning will be measured by microarray and deep sequencing respectively.

As for nucleosome positioning, Shivaswamy et al built a positive correlation between the placement of individual nucleosomes at the promoter and the accessibility of transcription factors (Shivaswamy et al., 2008). By measuring protein binding sites by ChIP-chip and compare them with deep sequencing results, before and after heat shock, they concluded that gene activation is mainly associated with nucleosome eviction and repression with nucleosome appearance. So I expect that if H3 tail deletion has any effect on the

transcription level of certain genes, these effects would be reflected by changes in the nucleosome positioning profiles.

I predict that for those genes within the euchromatin affected by H3 tail deletion, no matter positively or negatively, their transcription levels and nucleosome positioning in the single-tailed strain will be similar to that in the tailless strain, and will still be significantly different from that of wild-type. Because a single H3 tail may not be as fully functional to maintain normal level of gene transcription as both tails are, mainly due to the impaired enzymatic cooperativity and crosstalk between histone modifications. For those genes within the heterochromatin, their expression in the single-tailed strain might still be repressed, which is similar to the intact strain. Silenced chromatin forms an ordered, compact structure with continuously distributed Sir proteins (Grunstein, 1998). H3 tails play a relatively minor role in maintaining heterochromatin structure and silencing compared to H4 tails, which are required for nucleosome oligomerization to form compact chromatin fibers (Dorigo et al., 2003). A single H3 tail along with other histone tails may still provide sufficient binding sites for negatively charged proteins or DNA in adjacent nucleosomes. The highly condensed chromatin structure might not be disrupted and the silencing state would be maintained.

Histones can be modified at several residues, and each modification constitutes a signal that is read alone or in combination with others on the same or adjacent histones (Probst et al., 2009). It was observed that the H3

K9/14R allele produced the most dramatic telomeric silencing defect with the fewest H3 mutations (Kelly et al., 2000). And the acetylation of H3K9 and H3K14 is highest at the 5' ends of genes, which correlates with gene activity (Millar and Grunstein, 2006). With the new H3 heterodimer, it is possible to generate one-sided K9/14R mutations [K9/14R : K9/14], or one mutation for each tail [K9R : K14R], within each nucleosome. By measuring gene expression and silencing defects (Gottschling et al., 1990) for these two strains, they might show some different Cis vs. Trans patterns, e.g. the combination of K9/14R on the same tail has a greater effect than distributed onto two tails. More mutants such as [K9/14R : K9R], [K9/14R : K14R] and [K9/14R : K9/14R] could be generated to serve as control strains. These experiments will be useful for a deeper interpretation of the multiple-modification system.

In sum, the ability to manipulate the H3-H3 interaction that bridge the core histone tetramer enables us to determine if symmetrical H3s are required for a wide array of fundamental biological processes. The thesis work provided a new set of reagents and methods, which are likely to be useful for studies in any eukaryotic organism.

Supplement

Besides the above project of nucleosomal symmetry, I did some other work on Rtt109 during my graduate studies. In this section I will briefly introduce the background and show the results.

Histone acetylation, as one important class of the histone modifications, regulates diverse processes such as nucleosome assembly, gene activity, DNA repair and genomic stability in eukaryotes. Histone acetyltransferases (HATs) function within multi-subunit complex with accessory proteins which regulate enzymatic activity and substrate specificity (Carrozza et al., 2003). For example, the HAT Rtt109 require association with either one of the two histone chaperones, Vps75 or Asf1, for substrate selection and catalytic efficiency (Berndsen et al., 2008). Rtt109 acetylates lysine 56 on the newly synthesized H3 in yeast, and H3K56ac is absent in *asf1*Δ mutants but normal in *vps75*Δ mutants, indicating an essential role for Asf1 in the Rtt109-dependent acetylation of H3K56 (Driscoll et al., 2007). Vps75 co-purifies with Rtt109, and *vps75*Δ yeast cells display a reduction of acetylation level on K9, K23 and K27 of H3 (Berndsen et al., 2008; Burgess et al., 2010).

Our collaborator Dr. John Denu's group produced a model for the Rtt109-Vps75 complex based on X-ray crystallographic studies, and revealed two electrostatic interfaces between an Rtt109 molecule and a Vps75 dimer

(Figure 1). To assess the importance of this electrostatic interaction, two sets of amino-acid substitutions within Rtt109 (E374K / E378K and E299K / E300K / D301K) were generated. Steady-state kinetic analyses suggested that compared to wild-type Rtt109, Rtt109 variants with interface point substitutions had no significant change in substrate binding, overall affinity between Rtt109 and Vps75, or Asf1-dependent acetylation, but they lack the ability to be fully activated by Vps75.

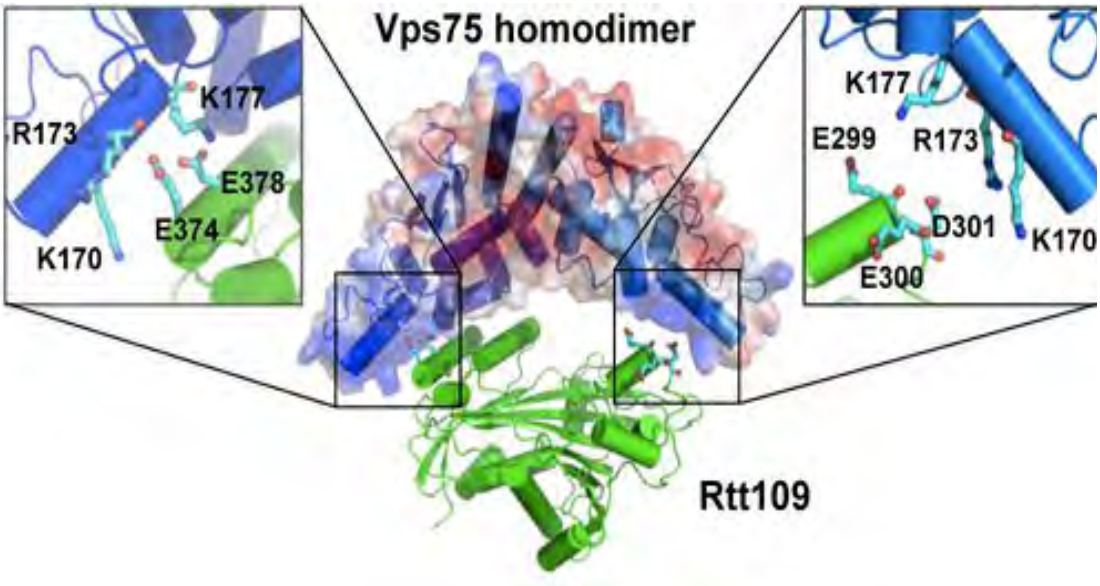

Figure 1 (Kolonko et al.): The proposed Rtt109–Vps75 complex interface. Acidic residues of Rtt109 (green) were proposed to interact with basic patches of Vps75 (blue overlaid with a vacuum electrostatics surface generated in MacPyMOL).

To investigate the *in vivo* effects of these substitutions, we generated yeast strains carrying the mutant *rtt109* alleles. They were grown either on synthetic

media (SC-Leu) as a positive control for cell growth or on rich media (YPD) containing camptothecin (CPT, 8 μM) to measure genotoxic stress resistance (Figure 2A). CPT covalently traps topoisomerase I, leading to double-stranded DNA breaks (Liu et al., 2000), making Rtt109-Asf1 (but not Rtt109-Vps75) stimulated histone deposition essential for survival (Li et al., 2009). Both Rtt109 variants as well as wildtype Rtt109 were able to restore CPT resistance to the *rtt109*Δ strain, suggesting that the acetylation of H3K56 by Rtt109-Asf1 is unaffected by the point substitutions on Rtt109-Vps75 interface.

We also examined the acetylation of H3 in these strains by immunoblotting (Figure 2B). Whole cell extracts of *rtt109*Δ and *rtt109Δgcn5*Δ strains carrying the plasmid-borne *RTT109* alleles were probed for acetylation at K56, K9 and K27 of H3. The latter strain was used to investigate acetylation at H3K9 and H3K27, as both Rtt109 and Gcn5 acetylate these sites (Burgess et al., 2010). In agreement with the genome stability data, both Rtt109 variants supported normal levels of H3K56 acetylation. Interestingly, although normal levels of H3K9 and H3K27 acetylation were observed in cells expressing wild type Rtt109 and the variant Rtt109 (E374K, E378K), the variant Rtt109 (E299K, E300K, D301K) reduced levels of K9 and K27 acetylation in the r*tt109Δgcn5Δ* strain. These findings were supported by immunoblotting titrations of each variant using the double knockout strain (Figure 2C, D).

Together, these results indicate that the Rtt109-Vps75 interfaces are unique to the functional interaction between Rtt109 and Vps75, and that the activation of Rtt109 by Asf1 is mediated through a distinct mechanism.

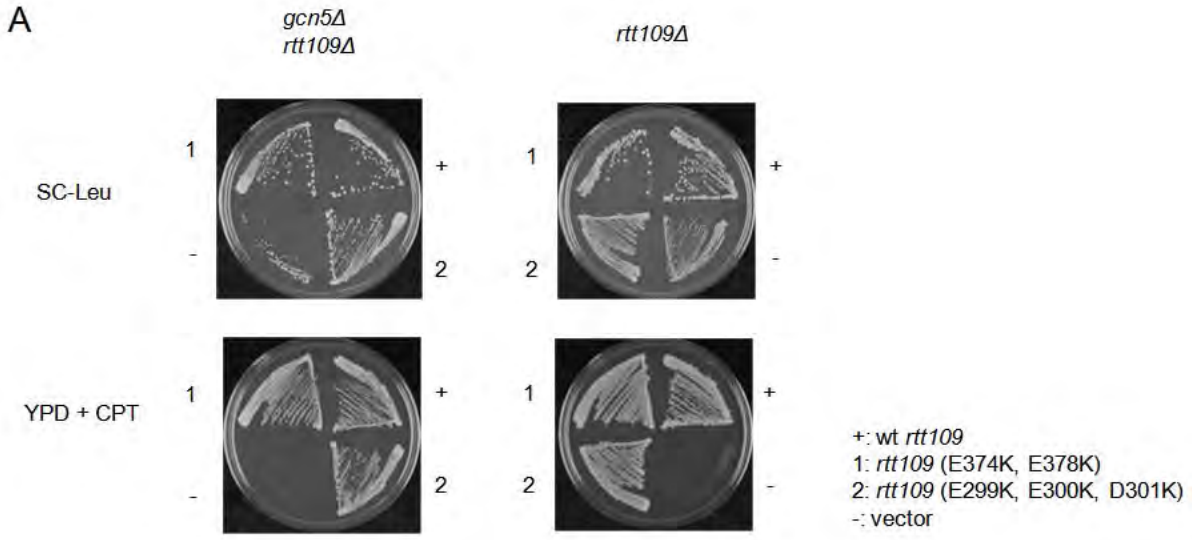

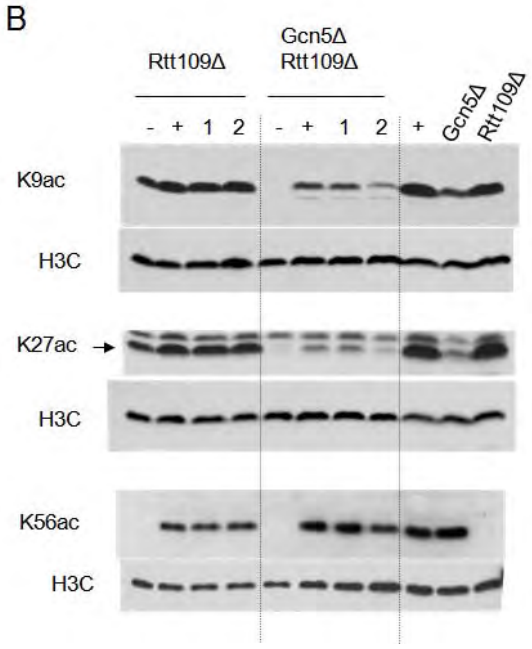

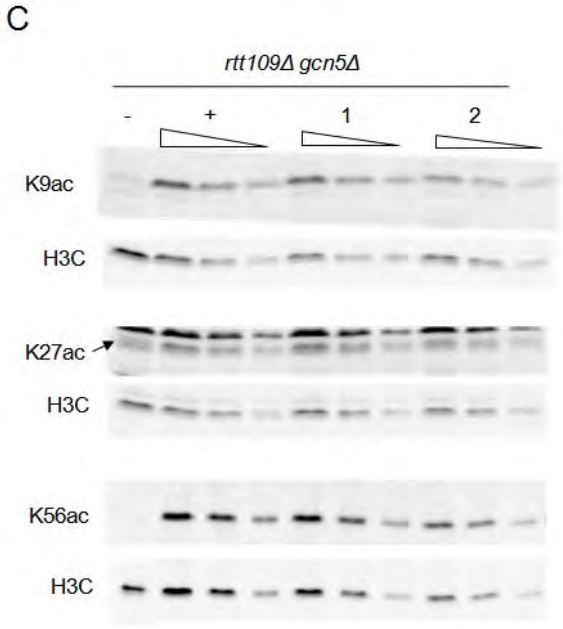

D

	wt	1	2
K9ac	1.14 ± 0.07	1.22 ± 0.02	0.77 ± 0.07 (-30%)
K27ac	1.3 ± 0.1	1.3 ± 0.1	1.03 ± 0.09 (-20%)
K56ac	1.1 ± 0.1	1.25 ± 0.08	1.27 ± 0.05

Figure 2: Variants of Rtt109 do not affect Rtt109-Asf1 activity in vivo. A) Wild-type Rtt109 and the Rtt109 variants are able to rescue genome stability of *rtt109*Δ and *rtt109Δgcn5*Δ strains. Yeast strains carrying the indicated *RTT109* alleles were plated either on rich media (YPD) containing 8 μM camptothecin (CPT) to indicate resistance to genotoxic stress, or on synthetic media (SC-Leu) as a positive control from growth. Plates were grown at 30°C for 3 days prior to photography. B) H3K56ac is not affected by the point substitutions in Rtt109; however, H3K9ac and H3K27ac are reduced in the *rtt109Δgcn5Δ* strain with the mutant Rtt109 allele (E299K, E300K, D301K). Whole cell alkaline lysis extracts of the indicated strains were analyzed by immunoblotting, with the indicated anti-acetyl histone antibodies and reprobed with anti-H3 antibody as the loading control. C) Whole-cell alkaline lysis extracts (7, 5, and 2.5 μl) were analyzed by immunoblotting with the indicated anti-acetyl histone antibodies and reprobed with anti-H3 antibody as the loading control. D) Immunoblots were quantitated using Image Gauge software. The anti-acetyl and anti-H3 histone signals were divided by the volume of lysis extract to yield signal/μl. The ratio of anti-acetyl histone signal/μl to anti-H3 signal/μl was calculated and is reported with standard error.

Materials and Methods

Antibodies

Anti-H3K9ac and K27ac (Upstate) and anti-H3 (Abcam) were from commercial suppliers.

Yeast strains

PKY4333 (*MAT*a; *leu2-3, 112; ura3-1; his3-11,15; trp1-1; ade2-1; can1-100; ADE2-VR; URA3-VIIL; rtt109Δ::kanMX*) and PKY4527 (*MAT*a; *leu2-3, 112; ura3-1; his3-11,15; trp1-1; ade2-1; can1-100; rtt109Δ::kanMX; gcn5Δ::TRP1; ADE2-VR*) in the W303 genetic background were transformed with the low-copy plasmids, either the *ARS-CEN, LEU2* vector pRS415 (-), or a pRS415 derivative containing the wild-type RTT109 gene (+) or the rtt109-E374K/E378K (1) or rtt109-E299K/E300K/D301K (2) alleles. Mutant *rtt109* alleles were generated by PCR mutagenesis and confirmed by sequencing.

Bibliography

Berndsen, C.E., Tsubota, T., Lindner, S.E., Lee, S., Holton, J.M., Kaufman, P.D., Keck, J.L., and Denu, J.M. (2008). Molecular functions of the histone acetyltransferase chaperone complex Rtt109-Vps75. Nature structural & molecular biology *15*, 948-956.

Boeke, J.D., Trueheart, J., Natsoulis, G., and Fink, G.R. (1987). 5-Fluoroorotic acid as a selective agent in yeast molecular genetics. Methods in enzymology *154*, 164-175.

Bolon, D.N., Grant, R.A., Baker, T.A., and Sauer, R.T. (2005). Specificity versus stability in computational protein design. In Proceedings of the National Academy of Sciences of the United States of America, pp. 12724-12729.

Burgess, R.J., Zhou, H., Han, J., and Zhang, Z. (2010). A role for Gcn5 in replication-coupled nucleosome assembly. Mol Cell *37*, 469-480.

Carrozza, M.J., Li, B., Florens, L., Suganuma, T., Swanson, S.K., Lee, K.K., Shia, W.J., Anderson, S., Yates, J., Washburn, M.P*., et al.* (2005). Histone H3 methylation by Set2 directs deacetylation of coding regions by Rpd3S to suppress spurious intragenic transcription. Cell *123*, 581-592.

Carrozza, M.J., Utley, R.T., Workman, J.L., and Cote, J. (2003). The diverse functions of histone acetyltransferase complexes. Trends Genet *19*, 321-329.

Dai, J., Hyland, E.M., Yuan, D.S., Huang, H., Bader, J.S., and Boeke, J.D. (2008). Probing nucleosome function: a highly versatile library of synthetic histone H3 and H4 mutants. Cell *134*, 1066-1078.

Dion, M.F., Kaplan, T., Kim, M., Buratowski, S., Friedman, N., and Rando, O.J. (2007). Dynamics of replication-independent histone turnover in budding yeast. Science (New York, NY *315*, 1405-1408.

Don, R.H., Cox, P.T., Wainwright, B.J., Baker, K., and Mattick, J.S. (1991). 'Touchdown' PCR to circumvent spurious priming during gene amplification. Nucleic acids research *19*, 4008.

Dorigo, B., Schalch, T., Bystricky, K., and Richmond, T.J. (2003). Chromatin fiber folding: requirement for the histone H4 N-terminal tail. Journal of molecular biology *327*, 85-96.

Driscoll, R., Hudson, A., and Jackson, S.P. (2007). Yeast Rtt109 promotes genome stability by acetylating histone H3 on lysine 56. Science (New York, NY *315*, 649-652.

Gottschling, D.E., Aparicio, O.M., Billington, B.L., and Zakian, V.A. (1990). Position effect at S. cerevisiae telomeres: reversible repression of Pol II transcription. Cell *63*, 751-762.

Grunstein, M. (1998). Yeast heterochromatin: regulation of its assembly and inheritance by histones. Cell *93*, 325-328.

Kelly, T.J., Qin, S., Gottschling, D.E., and Parthun, M.R. (2000). Type B histone acetyltransferase Hat1p participates in telomeric silencing. Mol Cell Biol *20*, 7051-7058.

Lee, J.S., Shukla, A., Schneider, J., Swanson, S.K., Washburn, M.P., Florens, L., Bhaumik, S.R., and Shilatifard, A. (2007). Histone crosstalk between H2B monoubiquitination and H3 methylation mediated by COMPASS. Cell *131*, 1084-1096.

Li, Q., Fazly, A.M., Zhou, H., Huang, S., Zhang, Z., and Stillman, B. (2009). The elongator complex interacts with PCNA and modulates transcriptional silencing and sensitivity to DNA damage agents. PLoS Genet *5*, e1000684.

Li, S., and Shogren-Knaak, M.A. (2008). Cross-talk between histone H3 tails produces cooperative nucleosome acetylation. Proceedings of the National Academy of Sciences of the United States of America *105*, 18243-18248.

Ling, X., Harkness, T.A., Schultz, M.C., Fisher-Adams, G., and Grunstein, M. (1996). Yeast histone H3 and H4 amino termini are important for nucleosome assembly in vivo and in vitro: redundant and position-independent functions in assembly but not in gene regulation. Genes Dev *10*, 686-699.

Liu, L.F., Desai, S.D., Li, T.K., Mao, Y., Sun, M., and Sim, S.P. (2000). Mechanism of action of camptothecin. Ann N Y Acad Sci *922*, 1-10.

Luger, K., Mader, A.W., Richmond, R.K., Sargent, D.F., and Richmond, T.J. (1997). Crystal structure of the nucleosome core particle at 2.8 A resolution. In Nature, pp. 251-260.

Mann, R.K., and Grunstein, M. (1992). Histone H3 N-terminal mutations allow hyperactivation of the yeast GAL1 gene in vivo. EMBO J *11*, 3297-3306.

Millar, C.B., and Grunstein, M. (2006). Genome-wide patterns of histone modifications in yeast. Nat Rev Mol Cell Biol *7*, 657-666.

Probst, A.V., Dunleavy, E., and Almouzni, G. (2009). Epigenetic inheritance during the cell cycle. Nat Rev Mol Cell Biol *10*, 192-206.

Sabet, N., Tong, F., Madigan, J.P., Volo, S., Smith, M.M., and Morse, R.H. (2003). Global and specific transcriptional repression by the histone H3 amino terminus in yeast. Proceedings of the National Academy of Sciences of the United States of America *100*, 4084-4089.

Santos-Rosa, H., Kirmizis, A., Nelson, C., Bartke, T., Saksouk, N., Cote, J., and Kouzarides, T. (2009). Histone H3 tail clipping regulates gene expression. Nature structural & molecular biology *16*, 17-22.

Shivaswamy, S., Bhinge, A., Zhao, Y., Jones, S., Hirst, M., and Iyer, V.R. (2008). Dynamic remodeling of individual nucleosomes across a eukaryotic genome in response to transcriptional perturbation. PLoS biology *6*, e65.

Sikorski, R.S., and Hieter, P. (1989). A system of shuttle vectors and yeast host strains designed for efficient manipulation of DNA in Saccharomyces cerevisiae. Genetics *122*, 19-27.

Suganuma, T., and Workman, J.L. (2008). Crosstalk among Histone Modifications. In Cell, pp. 604-607.

Thompson, J.S., Ling, X., and Grunstein, M. (1994). Histone H3 amino terminus is required for telomeric and silent mating locus repression in yeast. Nature *369*, 245-247.

Viggiani, C.J., and Aparicio, O.M. (2006). New vectors for simplified construction of BrdU-Incorporating strains of Saccharomyces cerevisiae. Yeast *23*, 1045-1051.